This document is a preprint of: Z. Li, R. Bomfin, I. Bizon Franco de Almeida et al., "Position-Driven Wireless Multipath Channel Simulator for Square-Shaped Environments," in Proceedings of 1st IEEE International Online Symposium on Joint Communications &S 2021), Virtual Conference, (pp. 1-6), Feb 2021. DOI:10.1109/JCS52304.2021.9376345
for publication, virtual, Feb. 2021. DOI: 10.1109/JCS52304.2021.9376345.

Position-Driven Wireless Multipath Channel Simulator for Square-Shaped Environments

Zhongju Li*, Roberto Bomfin*, Ivo Bizon Franco de Almeida*,
Ahmad Nimr†, Norman Franchi†, Gerhard Fettweis†
Vodafone Chair Mobile Communication Systems, Technische Universität Dresden, Germany
*{first name.last name}@ifn.et.tu-dresden.de
†{first name.last name}@tu-dresden.de

***Abstract*—In this paper, we propose an analysis of the wireless multipath channel in square-shaped environments. By considering propagation characteristics of the wireless transmission such as path-loss and reflections in this environment, we provide a wireless multipath channel generator that depends on transmitter and receiver position and can be easily integrated into numerical simulations. In order to demonstrate the validity of the proposed simulation framework, we provide a numerical analysis of the spatial channel correlation between two receivers over random positions of the transmitter in a defined area, which can be also treated as a performance indicator. Interestingly, the results show that the region where the transmitter is positioned has a large impact on the channel correlation. To corroborate our channel simulator, a blind energy detection based spectrum sensing has been implemented, where we show the influence of transmitter position and channel spatial correlation on the system performance.**

***Index Terms*—Deterministic channel model, multi-path channel simulator, channel spatial correlation, spectrum sensing**

I. Introduction

RECENTLY, a lot of attention has been drawn towards the challenges in wireless channel modeling techniques that accurately reflect the propagation characteristic related to different positions, i.e., a position-based channel model. In [1], the authors show that the position information is contained in the multipath channel, which can be used for localization. This fact indicates the need for a position-driven multipath channel simulator considering the environment for the research.

The classical channel modeling follows either deterministic or stochastic approaches. The stochastic approach is developed based on a broad set of data obtained via measurement campaigns. However, it is not able to offer the dependency of the channel on the absolute position of the transmitter and the receiver. On the other hand, the deterministic approach, such as the ray-tracing techniques [2], considers the exact physics of the wave propagation and surrounding environment for a particular situation.

Correspondingly, a position-based wireless channel simulator formulated as a function block, as illustrated in Fig. 1, is a valuable tool in designing algorithms that aim to exploit user position information. In [3], [4] the authors provide

This work was funded and supported by the project "Industrial Radio Lab Germany" under contract 16KIS1010K, funded by the Federal Ministry of Education and Research, Germany.

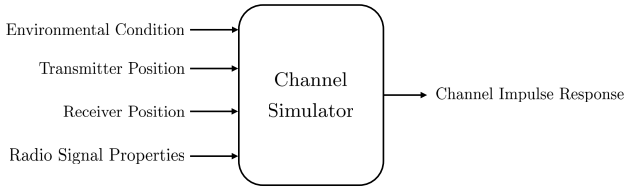

Fig. 1: Concept of position-based channel simulator.

analysis using the image source method for the geometrical acoustic simulation. However, they use an approximation of the reflection coefficient. Also, they provide an analysis of the continuous-time channel model for the acoustic signal without considering the impact of sampling and signal bandwidth. In [5], [6] the authors present the ray-tracing model for the tunnel environment, which is similar to the scenario considered in this paper. However, they approach the modeling from the electric wave propagation point of view and prove that the electric field within a hollow dielectric waveguide can be represented by a ray summation based on the ray-tracing method. Therefore, they do not provide the multipath channel analysis in the given environment setup.

Motivated by these points, we propose a methodology for the realization of position-based multipath channel simulator for rectangular-shaped environments. As an initial step, we apply this on a rectangular-shaped environment without obstacles and with smooth wall surface. The simulator is able to integrate large-scale temporal as well as spatial influences on the propagation of radio signals, which reflect the most important characteristics of a multipath channel model. Comparing with [3], [4], we consider the exact reflection coefficient by respecting the angle of incident of the transmitted signal. Moreover, we provide the modeling of the wireless channel given the bandwidth of the transmitted signal.

As application of using the fast generated channel impulse response (CIR), one can perform statistical analysis given the possible regions of the transmitter and the receiver, as well as the geometry of the environment. The analysis then can be used, as we show in section IV, for the system performance optimization, e.g., for the optimization of the sensor grid arrangement. For instance, we present a statistical application

© 2021 IEEE. Personal use of this material is permitted. Permission from IEEE must be obtained for all other uses, in any current or future media, including reprinting/republishing this material for advertising or promotional purposes, creating new collective works, for resale or redistribution to servers or lists, or reuse of any copyrighted component of this work in other works.

This document is a preprint of: Z. Li, R. Bomfin, I. Bizon Franco de Almeida et al., "Position-Driven Wireless Multipath Channel Simulator for Square-Shaped Environments," in Proceedings of 1st IEEE International Online Symposium on Joint Communications & Sensing (JC&S 2021), Virtual Conference, (pp. 1-6), Feb 2021. DOI:10.1109/JCS52304.2021.9376345.

of our simulator by computing the spatial correlation of two sensors numerically, where we fix the position of the sensors and generate the source position randomly in a given region. The spatial correlation, which can only be obtained by using a position-based channel simulator or by measurement, plays a significant role on the performance of spectrum sensing algorithms, as we will show in this paper. As an application example of the spatial correlation, we employ our simulator to a cooperative energy detection based spectrum sensing [7], in which we show that the performance depends on the transmitter position due to different spatial correlation. Concretely, for the use cases where the system performance is also required for the worst-case scenario, it is not sufficient to only examine the average performance. Moreover, the spatial correlation can be also treated as a property of the environment, which can be set as a prior knowledge for the localization.

The reminder of the paper is organized as follows: Section II presents a background on the wave propagation and wireless multipath channel modeling. Section III describes the proposed position-driven multipath channel model with implementation remarks. Section IV presents the numerical simulation of the proposed implementation, where a statistical analysis is shown, followed by an application example for the spectrum sensing. Finally, section V concludes the paper and provides some outlook.

II. Basic Wireless Channel Characteristics

A. Wave propagation model

Suppose the transmitter and receiver both use an omnidirectional antenna, and the transmitted wave propagates within a given lossless medium. In that case, the ratio between the received and transmitted power P_r and P_t is then subjected to the free-space propagation loss given in the logarithmic scale as

$$FL(d) = \frac{P_r}{P_t} = 20\log\left(\frac{\lambda}{4\pi d}\right) + 10\log(G_t) + 10\log(G_r), \quad (1)$$

where G_t and G_r are the gains of the transmitter and receiver antenna, $\lambda = c/f$ is the wavelength in meters, being c the speed of light and f the carrier frequency in Hertz. Lastly, d is the distance traveled by the wave in meters.

However, when the wave propagates to a boundary of two different media, i.e., the media have different permeabilities ϵ and permittivities μ, the wave is then reflected into the same medium where it comes, and refracted into the other medium. This phenomenon is depicted in Fig. 2, where $\boldsymbol{E}$ is the electric vector field. In this paper, we focus on the reflected wave, since the transmitted wave shown in Fig. 2 will not reach the receive antenna. Due to the reflection, the amplitude of the reflected wave E_r differs from the incident wave E_i. The ratio is expressed by the reflection coefficient $R = E_r/E_i$. The reflection coefficient of p-polarized/s-polarized wave is

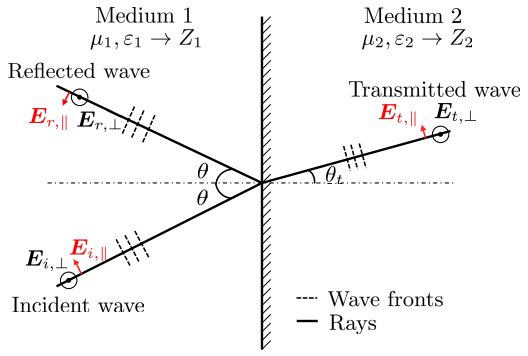

Fig. 2: Plane wave incident on a medium boundary.

respectively given by [8]

$$R_{\parallel/\perp}(\theta) = \frac{Z_{1/2}\cos\theta - Z_{2/1}\sqrt{1-\left(\frac{Z_2}{Z_1}\right)^2\sin^2\theta}}{Z_{2/1}\sqrt{1-\left(\frac{Z_2}{Z_1}\right)^2\sin^2\theta} + Z_{1/2}\cos\theta}, \quad (2)$$

where Z_j is the wave impedance defined by the media, $\parallel$ indicates the p-polarization, $\perp$ the s-polarization, and θ is the angle of incident.

B. Multipath channel model

Since the transmitter and receiver are surrounded by walls or other objects, the received signal consists of many replicas of the transmitted signal with different time delays due to the reflection [9]. Therefore, the continuous-time baseband equivalent multipath CIR, consists of L paths, is formulated as [10]

$$h(t) = \sum_{l=0}^{L-1} \alpha_l e^{j\varphi_l}\delta(t-\tau_l), \quad (3)$$

where the $\delta(\cdot)$ is the Dirac function, α_l, $\tau_l = \frac{d_l}{c}$, and $\varphi_l = 2\pi\frac{d_l}{\lambda} = 2\pi f\tau_l$ are the gain, the delay, and the phase rotation of the l-th path, respectively. Each individual path is attenuated due to free-space propagation and reflection loss. For example, a path with distance d_l and reflected once by the wall, the gain in logarithmic scale is given by

$$\alpha_l = FL(d_l) - 20\log\left(R(\theta)\right). \quad (4)$$

In practice, setting the exact values of α_l, τ_l, and φ_l for a given environment is not possible. Those parameters depend on the physical properties of the antennas, material of the reflecting objects, propagation medium, etc. Thus, for the purpose of simulating the wireless channel, a common approach is to define those parameters based on statistical models, e.g., Rayleigh based channel, which does not necessarily capture the relevant aspects of the channel, e.g., spatial correlation. In the following section, we propose a simple approach to determine α_l, τ_l and φ_l in (3) for a rectangular-shaped environment.

© 2021 IEEE. Personal use of this material is permitted. Permission from IEEE must be obtained for all other uses, in any current or future media, including reprinting/republishing this material for advertising or promotional purposes, creating new collective works, for resale or redistribution to servers or lists, or reuse of any copyrighted component of this work in other works.

This document is a preprint of: Z. Li, R. Bomfin, I. Bizon Franco de Almeida et al., “Position-Driven Wireless Multipath Channel Simulator for Square-Shaped Environments,” in Proceedings of 1st IEEE International Online Symposium on Joint Communications & Sensing (JC&S 2021), Virtual Conference, (pp. 1-6), Feb 2021. DOI:10.1109/JCS52304.2021.9376345
for publication, virtual, Feb. 2021. DOI: 10.1109/JCS52304.2021.9376345.

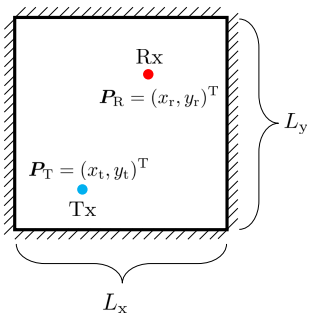

Fig. 3: Environmental setup of the simulator.

III. Proposed Multi-path Channel Simulator

The deterministic channel model based on ray tracing techniques has the advantage of providing the channel dependency on the position of the transmitter $\boldsymbol{P}_{\mathrm{T}}$ and receiver $\boldsymbol{P}_{\mathrm{R}}$ considering the environment around them. Our simulator focuses on a rectangular-shaped environment, e.g, in a two-dimensional empty rectangular-shaped room with four walls. Additionally, we assume both the transmitter and receiver employ omnidirectional antennas. Fig. 3 depicts the environment model setup of the simulator, where the receiver, marked as Rx, is located at the position $\boldsymbol{P}_{\mathrm{R}} = (x_{\mathrm{r}}, y_{\mathrm{r}})$, the width and the length of the two-dimensional room are L_{x} and L_{y}. The Tx represents the transmitter. In a sensing setup, the Tx is interpreted as the signal source and Rx as the sensor.

Additionally, we assume the walls of the room have smooth surface, i.e., they have surface features that are small compared to the used wavelength λ. The walls then act like mirrors [8]. The reflection coefficient is given by (2). Furthermore, the model considers only the paths which can reach the receiver with significant power, to reduce the computational complexity. Fig. 4 presents an example of the reflected paths from the walls of the room considering only the paths that are reflected once. Note that, according to the assumption about the environmental setup and image theory, if we focus on the sensor, we can define a virtual room with a virtual sensor inside for each wall. One can also focus on the source and define thus virtual source. The position of the virtual sensor is symmetric to the sensor regarding the corresponding

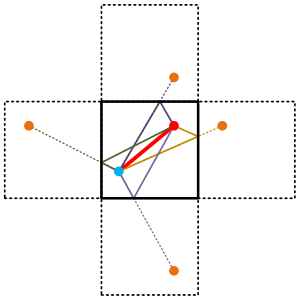

Fig. 4: Example of reflected paths with one reflection.

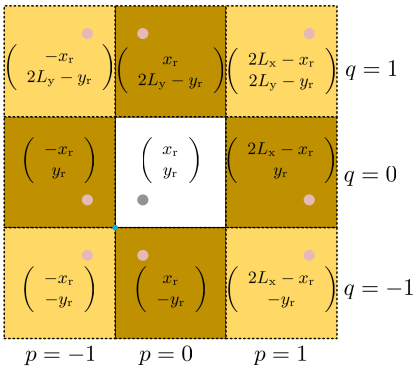

Fig. 5: Example of the virtual sensors location.

wall. The distance that the signal propagates along a path considering the reflection is equal to the distance from the source to the corresponding virtual sensor. For our setup, the virtual sensor regarding the bottom edge then has position in the coordinate $\boldsymbol{P}_{\mathrm{R}}^{\prime(0,-1)} = (x_{\mathrm{r}}, -y_{\mathrm{r}})^{\mathrm{T}}$. Similarly, one can find the virtual sensor for the wall on top, left, and right with coordinate $\boldsymbol{P}_{\mathrm{R}}^{\prime(0,1)} = (x_{\mathrm{r}}, 2L_{\mathrm{y}} - y_{\mathrm{r}})^{\mathrm{T}}$, $\boldsymbol{P}_{\mathrm{R}}^{\prime(-1,0)} = (-x_{\mathrm{r}}, y_{\mathrm{r}})^{\mathrm{T}}$, and $\boldsymbol{P}_{\mathrm{R}}^{\prime(1,0)} = (2L_{\mathrm{x}} - x_{\mathrm{r}}, y_{\mathrm{r}})^{\mathrm{T}}$. For the paths, which have more than one reflection with the walls, one can add virtual rooms and sensors and connect transmitter with virtual sensors to find them. The problem of determining the propagation paths is then converted into finding the position of the virtual sensors given by

$$\boldsymbol{P}_{\mathrm{R}}^{\prime(p,q)} = (x_p', y_q')^{\mathrm{T}}, \tag{5}$$

and the number of reflections (N_x, N_y), considering the angle of incident $\theta_{p,q}^{x}$ and $\theta_{p,q}^{y}$, to reach the virtual sensor in the corresponding virtual room marked with index (p, q). Fig. 5 depicts the position of the virtual sensors in some of the virtual rooms. The coordinate of the virtual sensor position is then represented by

$$\begin{aligned} x_p' &= 2\,\mathrm{int}\left(\frac{p}{2} + 1\right) L_{\mathrm{x}} + (-1)^p x_{\mathrm{r}} \\ y_q' &= 2\,\mathrm{int}\left(\frac{q}{2} + 1\right) L_{\mathrm{y}} + (-1)^q y_{\mathrm{r}}, \end{aligned} \tag{6}$$

where $\mathrm{int}(\frac{x}{y})$ returns the quotient of the division $\frac{x}{y}$. The analysis of the coordinate of the virtual sensors is also given in [3]. As mentioned before, another essential feature of the virtual room to be determined is the number of reflections that the radio signal experienced to reach the virtual sensor in the corresponding virtual room, as shown in Fig. 6. The number of reflections depends on how many walls and virtual walls the signal penetrates to reach the virtual sensor from the source. The total number of reflections is given by the number at the top in each virtual room in Fig. 6. Additionally, we consider the reflection with the wall in the x- and y-direction separately. Since for a certain path from the source to the virtual sensor in the virtual room (p, q), all the angles of incident of the wave with walls in the same direction, i.e, in the x- or y-direction, are identical. The angles are defined as $\theta_{p,q}^{x}$

© 2021 IEEE. Personal use of this material is permitted. Permission from IEEE must be obtained for all other uses, in any current or future media, including reprinting/republishing this material for advertising or promotional purposes, creating new collective works, for resale or redistribution to servers or lists, or reuse of any copyrighted component of this work in other works.

This document is a preprint of: Z. Li, R. Bomfin, I. Bizon Franco de Almeida et al., "Position-Driven Wireless Multipath Channel Simulator for Square-Shaped Environments," in Proceedings of 1st IEEE International Online Symposium on Joint Communications & Sensing (JC&S 2021), Virtual Conference, (pp. 1-6), Feb 2021. DOI:10.1109/JCS52304.2021.9376345.

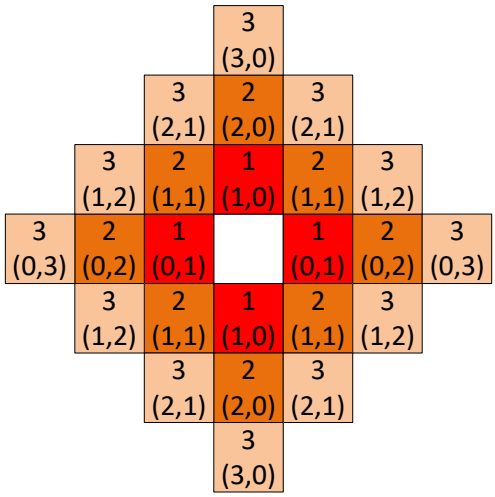

Fig. 6: Number of reflections in the certain virtual room.

and $\theta^y_{p,q}$ as mentioned before. Thus, the number of reflections with the walls in the x- and y-direction is denoted by a pair $(N_x, N_y) = (|p|, |q|)$ at the bottom in each virtual room in Fig. 6. Note that the number of actual sources and sensors is not limited to one. The system with more sources and/or more sensors is a superposition of multiple independent systems with one source and sensor. Moreover, the extension to 3D is easily achievable by reshaping the room into cuboid shape and adding cuboid virtual rooms around it. The coordinate in the third dimension is given by

$$z'_k = 2\,\mathrm{int}\left(\frac{k}{2}+1\right)L_\mathrm{z} + (-1)^k z_\mathrm{r}, \tag{7}$$

where k and L_z are the virtual room index and room height in the third dimension.

As another feature of the simulator, one can configure the bandwidth of the channel assuming the receiver and/or transmitter has only limited bandwidth. Interpolation with different time-domain filters can be implemented. To address the sampling with limited bandwidth in the time-domain, a *Sinc* shape filter $\mathrm{sinc}(x) = \frac{\sin(\pi x)}{\pi x}$ can be applied. Then, the discrete time baseband equivalent CIR considering multipath propagation and given bandwidth B in Hz is denoted as

$$h_{\boldsymbol{P}_\mathrm{T},\boldsymbol{P}_\mathrm{R}}[n] = \sum_{p=0}^{P-1}\sum_{q=0}^{Q-1} \alpha(d_{p,q})\mathrm{e}^{\mathrm{j}\varphi(d_{p,q})}\mathrm{sinc}\left[B\left(\frac{n}{B}-\frac{d_{p,q}}{c}\right)\right], \tag{8}$$

where $\varphi(d_{p,q}) = 2\pi d_{p,q}/\lambda$ and $d_{p,q} = \|\boldsymbol{P}_\mathrm{T} - \boldsymbol{P}_\mathrm{R}^{\prime(p,q)}\|$ being the distance between source and the corresponding sensor or virtual sensor. Furthermore, the path gain $\alpha(d_{p,q})$ in logarithmic scale considering the free-space propagation and reflections, is given by

$$\begin{aligned}\alpha(d_{p,q}) = {} & 20\log\left(\frac{\lambda}{4\pi d_{p,q}}\right) \\ & - N_x 20\log\left(R(\theta^x_{p,q})\right) - N_y 20\log\left(R(\theta^y_{p,q})\right).\end{aligned} \tag{9}$$

IV. Numerical Results

A. Statistical channel features: spatial correlation

As already mentioned in the previous sections, one of the relevant aspects of our simulator is to consider a spatial correlation of the channel, which is typically very hard to model [11]. Thus, in the following we numerically assess the spatial correlation produced by our model.

Firstly, we assume that the transmitter position is distributed within the area $\boldsymbol{P}_\mathrm{T} \in \{(x_\mathrm{T}, y_\mathrm{T}) | x_\mathrm{a} \leqslant x_\mathrm{T} < x_\mathrm{b}, y_\mathrm{a} \leqslant y_\mathrm{T} < y_\mathrm{b}\}$ uniformly. Then, we define the normalized spatial channel correlation for two different receiver positions, $\boldsymbol{P}_{\mathrm{R}_1}$ and $\boldsymbol{P}_{\mathrm{R}_2}$ as

$$C(\boldsymbol{P}_{\mathrm{R}_1}, \boldsymbol{P}_{\mathrm{R}_2}) = \frac{1}{\sqrt{E_1 E_2}\Delta_x\Delta_y}\int_{x_\mathrm{a}}^{x_\mathrm{b}}\int_{y_\mathrm{a}}^{y_\mathrm{b}} \boldsymbol{h}^\mathrm{H}_{\boldsymbol{P}_\mathrm{T},\boldsymbol{P}_{\mathrm{R}_1}} \boldsymbol{h}_{\boldsymbol{P}_\mathrm{T},\boldsymbol{P}_{\mathrm{R}_2}} \mathrm{d}x_\mathrm{T}\mathrm{d}y_\mathrm{T}, \tag{10}$$

where $\Delta_x = x_\mathrm{b} - x_\mathrm{a}$, $\Delta_y = y_\mathrm{b} - y_\mathrm{a}$, and

$$E_i = \frac{1}{\Delta_x\Delta_y}\int_{x_\mathrm{a}}^{x_\mathrm{b}}\int_{y_\mathrm{a}}^{y_\mathrm{b}} \boldsymbol{h}^\mathrm{H}_{\boldsymbol{P}_\mathrm{T},\boldsymbol{P}_{\mathrm{R}_i}} \boldsymbol{h}_{\boldsymbol{P}_\mathrm{T},\boldsymbol{P}_{\mathrm{R}_i}} \mathrm{d}x_\mathrm{T}\mathrm{d}y_\mathrm{T} \tag{11}$$

denotes the power of the the i-th channel. Note that the spatial correlation defined in (10) is generalized for any area where the transmitter can be located. Thus, for a spectrum sensing application with multiple sensors, it is beneficial to check the correlation between different Rx positions, since two uncorrelated channels provide more diversity, i.e., better sensing performance [7]. Additionally, for a CIR-based localization, the correlation can be set as prior knowledge to improve the location estimation.

We evaluate equation (10) numerically in order to provide a statistical analysis about our simulator. We assume a room with size $L_\mathrm{x} = L_\mathrm{y} = 10$ meters. The location of the two sensors are set as $\boldsymbol{P}_{\mathrm{R}_1} = (5, 5 - \Delta_d/2)$ and $\boldsymbol{P}_{\mathrm{R}_2} = (5, 5 + \Delta_d/2)$, such that they are located at the center of the room and are spaced by the Euclidean norm $\|\boldsymbol{P}_{\mathrm{R}_1} - \boldsymbol{P}_{\mathrm{R}_2}\| = \Delta_d$ meters. In order to show the impact of having the transmitter localized within a specific area, we define the correlations i) C_room with $(x_\mathrm{a} = 0, y_\mathrm{a} = 0)$ and $(x_\mathrm{b} = 10, y_\mathrm{b} = 10)$ assuming that the transmitter can be located at any area in the room, and ii) C_area, where the transmitter is restricted to the area $(x_\mathrm{a} = 4, y_\mathrm{a} = 0)$ and $(x_\mathrm{b} = 5, y_\mathrm{b} = 1)$, as illustrated in Fig. 8.

The evaluation of (10) for different Tx areas and Δ_d is presented in the Fig. 7. Interestingly, the outcomes show that although the average correlation C_room drops with a higher slope than C_area, C_area remains at a high value even at a distance of 2 meters, which indicates that the spatial correlation of both channels depends on the possible positions of the transmitter. As for the application of sensors arrangement optimization for spectrum sensing, according to this result, one should consider to rotate the two sensors regarding the center of the room or add more sensors in the x-direction to ensure the performance in all areas in the monitoring region, since the correlation in the certain area barely changes by separating the two sensors. This result also highlights that the location based correlation information is essential, if one

© 2021 IEEE. Personal use of this material is permitted. Permission from IEEE must be obtained for all other uses, in any current or future media, including reprinting/republishing this material for advertising or promotional purposes, creating new collective works, for resale or redistribution to servers or lists, or reuse of any copyrighted component of this work in other works.

This document is a preprint of: Z. Li, R. Bomfin, I. Bizon Franco de Almeida et al., “Position-Driven Wireless Multipath Channel Simulator for Square-Shaped Environments,” Proceedings of 1st IEEE International Online Symposium on Joint Communications & Sensing (JC&S 2021), Virtual Conference, (pp. 1-6), Feb 2021. DOI:10.1109/JCS52304.2021.9376345.
for publication, virtual, Feb. 2021. DOI: 10.1109/JCS52304.2021.9376345.

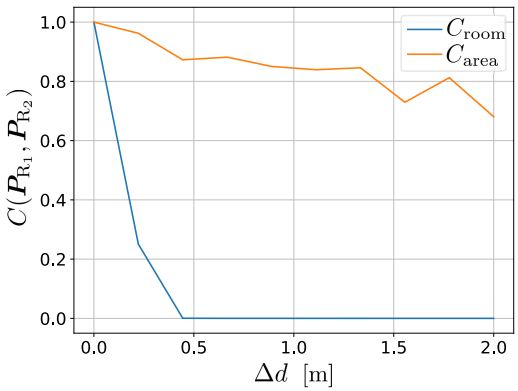

Fig. 7: Channel correlation regarding the distance Δ_d, $f_c = 2.4\,\text{GHz}$, $B = 15\,\text{kHz}$, $L_\text{x} = L_\text{y} = 10\,\text{m}$.

considers not only the average system performance but also the system performance at the worse case.

For a better understanding of the correlation at different locations in the room, we divide the room into 100 equal size areas of 1m × 1m as depicted in Fig. 8. We fix the Rx positions to $\boldsymbol{P}_{\text{R}_1} = (5, 4.75)$ and $\boldsymbol{P}_{\text{R}_2} = (5, 5.25)$ and compute the correlation in (10) for all areas. Clearly, the Tx position has a large impact on the channel correlation. This information can be used as a map for the system performance. In the next subsection, we show how this phenomenon impacts a spectrum sensing application. As for the CIR-based localization application, the correlation can be used as prior knowledge for initializing or improving the accuracy of the localization estimation.

B. Application example: spectrum sensing

The goal of this subsection is to provide an application example for the position dependent channel simulator presented in this paper. For this purpose, we consider a simple blind energy detection based spectrum sensing application

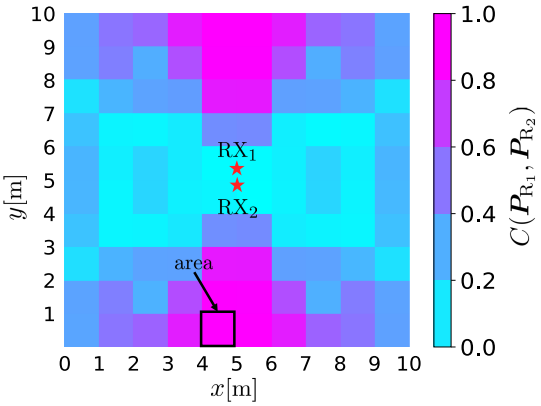

Fig. 8: Correlation heat map of the two channels $\mathbf{h}_1$ and $\mathbf{h}_2$, $f_c = 2.4\,\text{GHz}$, $B = 15\,\text{kHz}$, $\Delta_d = 0.5\,\text{m}$, $L_\text{x} = L_\text{y} = 10\,\text{m}$.

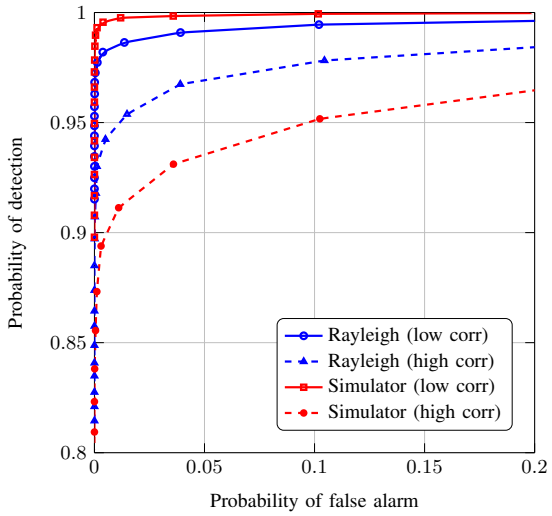

Fig. 9: Receiver Operating Characteristic (ROC) curve of the energy detection based spectrum sensing application.

under correlated channel [7]. In addition to our channel model presented in the previous subsection, we also consider a regular Rayleigh distributed channel for comparison, which is typically assumed in simulations.

As in the Subsection IV-A, we consider two sensors positioned at the center of the grid depicted in Fig. 8, with coordinates $\boldsymbol{P}_{\text{R}_1} = (5, 4.75)$ and $\boldsymbol{P}_{\text{R}_2} = (5, 5.25)$, i.e., with a distance of $\Delta_d = 0.5\,\text{m}$. The transmitter is positioned in two possible regions, i) $(x_\text{a} = 4, y_\text{a} = 0)$ and $(x_\text{b} = 5, y_\text{b} = 1)$ which produces a high correlation of 0.9 as indicated in the Fig. 8, and ii) $(x_\text{a} = 1, y_\text{a} = 4)$ and $(x_\text{b} = 2, y_\text{b} = 5)$, which produces a low correlation 0.06, see Fig. 8. For simplicity, we consider that the transmitter has a narrow band signal of $B = 15\,\text{kHz}$. Thus, the impulse responses of $\boldsymbol{h}_1$ and $\boldsymbol{h}_2$ are merged into one channel tap. In addition, we normalize the channel coefficients to a unitary averaged gain $1/2E[|\boldsymbol{h}_1|^2 + |\boldsymbol{h}_2|^2] = 1$. Notice that for the position dependent channel, in general $E[|\boldsymbol{h}_1|^2] \neq E[|\boldsymbol{h}_2|^2]$ because the transmitter can be closer to one of the sensors.

For the typical Rayleigh channel, we consider the one tap channel responses $\boldsymbol{h}_1$ and $\boldsymbol{h}_2$ with envelope being Rayleigh distributed with unitary power, and the phase being uniformly distributed between 0 and 2π. We set the same correlation defined by our simulation, i.e., $E[\boldsymbol{h}_1^\text{H}\boldsymbol{h}_2] = 0.9$ and $E[\boldsymbol{h}_1^\text{H}\boldsymbol{h}_2] = 0.06$ for the high and low correlation cases, respectively.

We consider a centralized spectrum sensing scheme, where the received signal of both sensors is available at the fusion center. The received signal of both sensors is defined by the matrix $\boldsymbol{Y} \in \mathbb{C}^{N\times 2}$ under the hypotheses $\mathcal{H}_0$ and $\mathcal{H}_1$

$$\mathcal{H}_0: \quad \boldsymbol{Y} = \boldsymbol{W} \tag{12}$$

$$\mathcal{H}_1: \quad \boldsymbol{Y} = \boldsymbol{x}\boldsymbol{H} + \boldsymbol{W}, \tag{13}$$

where $\mathcal{H}_0$ denotes the hypothesis where the transmit signal

© 2021 IEEE. Personal use of this material is permitted. Permission from IEEE must be obtained for all other uses, in any current or future media, including reprinting/republishing this material for advertising or promotional purposes, creating new collective works, for resale or redistribution to servers or lists, or reuse of any copyrighted component of this work in other works.

This document is a preprint of: Z. Li, R. Bomfin, I. Bizon Franco de Almeida et al., "Position-Driven Wireless Multipath Channel Simulator for Square-Shaped Environments," in Proceedings of 1st IEEE International Online Symposium on Joint Communications & Sensing (JC&S 2021), Virtual Conference, (pp. 1-6), Feb 2021. DOI:10.1109/JCS52304.2021.9376345
for publication, virtual, Feb. 2021. DOI: 10.1109/JCS52304.2021.9376345.

is absent, while $\mathcal{H}_1$ denotes the hypothesis in which the transmit signal is present. The matrix $\boldsymbol{W} \in \mathbb{C}^{N\times 2}$ is composed by independent and identically distributed (i.i.d.) Gaussian random variables to model the additive white Gaussian noise (AWGN) with power σ^2. The first and second columns of $\boldsymbol{W}$ represent the AWGN noise of the first and second sensor, respectively. The column vector $\boldsymbol{x} \in \mathbb{C}^{N\times 1} \sim \mathcal{CN}(0, \rho\boldsymbol{I})$ is the transmit signal which is assumed to be composed by i.i.d. Gaussian random variables with power ρ, which is present only in $\mathcal{H}_1$. Additionally, $\boldsymbol{H} = [\boldsymbol{h}_1\ \boldsymbol{h}_2] \in \mathbb{C}^{1\times 2}$ is a row vector containing the channel responses of the first and second sensors, respectively. Finally, N is the amount of collected samples at both sensors.

The goal of the spectrum sensing is to determine whether there is a user transmitting in the spectrum or not. In our case, we consider an energy detection algorithm for simplicity, where the decision variable is calculated as

$$T = \frac{1}{2N}\sum_{i=1}^{2}\sum_{j=1}^{N}|\boldsymbol{Y}[i,j]|^2. \tag{14}$$

Thus, the hypothesis test is performed by comparing the decision variable T to a threshold γ, such that

$$\begin{aligned} &\text{for } T<\gamma, \quad \text{decide in favor of } \mathcal{H}_0 \\ &\text{for } T>\gamma, \quad \text{decide in favor of } \mathcal{H}_1. \end{aligned} \tag{15}$$

Based on the decision algorithm defined by (15), we consider the widely used performance metrics

$$\begin{aligned} P_{\mathrm{d}} &= \Pr[\text{decision} = \mathcal{H}_1|\mathcal{H}_1] = \Pr[T>\gamma|\mathcal{H}_1] \\ P_{\mathrm{fa}} &= \Pr[\text{decision} = \mathcal{H}_1|\mathcal{H}_0] = \Pr[T>\gamma|\mathcal{H}_0], \end{aligned} \tag{16}$$

where P_{d} is the probability of detection and P_{fa} is the probability of false alarm, which define the receiver operating characteristic (ROC) curve.

The results are depicted in Fig. 9, where we consider that the sensors collect $N = 200$ samples, with a low signal to noise ratio (SNR) of $10\log_{10}\rho/\sigma^2 = 0$ dB. First of all, we observe that the low correlation curves for both simulator and Rayleigh based channels provide a better spectrum sensing performance. This behavior has already been demonstrated in [7], and is explained by the fact that if one channel happens to be with low power, the other channel can have sufficient power to still correctly detect the presence of the transmitter. Secondly, we observe that our simulator provides a significant different performance in comparison to the typical Rayleigh channel, since the Rayleigh model only describes the averaged channel according to the statistics. More importantly, we have mapped the high and low correlation channels to a particular area where the transmission can be located. This mapping can not be achieved with statistical channel models. The results indicate that the position of the transmitter in a given environment also has impact on the channel statistics and they will impact in the performance of applications such as spectrum sensing or localization. Thus, this spatial behavior should be investigated using position-driven simulators.

V. Conclusion and Outlook

In this paper, we provide a methodology for position-driven wireless multipath channel and apply it to rectangular-shaped environments. Compared with the geometrical acoustic channel model, we provide the exact reflection coefficient regarding the angle of incident and show that this can be easily applied by analyzing the reflections. Additionally, our proposed multipath channel simulator is able to generate the discrete time CIR for a bandlimited signal.

We show by means of examples how essential it is to consider the position-driven CIR rather than a statistical one for the simulation of a CIR-based localization algorithm and the evaluation of the system performance such as spectrum sensing system in a given environment. In particular, we present a statistical analysis of the spatial correlation using our channel simulator, where the transmitter position has a considerable impact. Moreover, we show that the spatial correlation can be treated as a property of the environment or prior knowledge for a particular application. As an application example, we consider an energy detection based spectrum sensing scheme using two sensors, where the transmitter position had a considerable impact on the performance. For that, we imply that the knowledge obtained by the channel simulator can be used for optimizing the sensors arrangement for this application.

The simulator helps as an alternative to realistic costly measurement, however, several realistic assumptions such as scattering, and blockage need to be considered and validated with realistic measurement. This will be subjected to future works.

References

[1] K. Witrisal, P. Meissner, E. Leitinger, Y. Shen, C. Gustafson, F. Tufvesson, K. Haneda, D. Dardari, A. F. Molisch, A. Conti *et al.*, "High-accuracy localization for assisted living: 5g systems will turn multipath channels from foe to friend," *IEEE Signal Processing Magazine*, vol. 33, no. 2, pp. 59–70, 2016.

[2] D. I. Laurensen, "Indoor radio channel propagation modelling by ray tracing techniques," Ph.D. dissertation, University of Edinburgh, 1994.

[3] J. B. Allen and D. A. Berkley, "Image method for efficiently simulating small-room acoustics," *The Journal of the Acoustical Society of America*, vol. 65, no. 4, pp. 943–950, 1979.

[4] F. Brinkmann, V. Erbes, and S. Weinzierl, *Extending the closed form image source model for source directivity*, 2018.

[5] C. Zhou and J. Waynert, "The equivalence of the ray tracing and modal methods for modeling radio propagation in lossy rectangular tunnels," *IEEE Antennas and Wireless Propagation Letters*, vol. 13, pp. 615–618, 2014.

[6] C. Zhou, "Ray tracing and modal methods for modeling radio propagation in tunnels with rough walls," *IEEE transactions on antennas and propagation*, vol. 65, no. 5, pp. 2624–2634, 2017.

[7] R. Bomfin and R. de Souza, "Performance of centralized data-fusion cooperative eigenvalue-based spectrum sensing under correlated shadowed fading," in *2015 International Workshop on Telecommunications (IWT)*, 2015, pp. 1–6.

[8] S. R. Saunders, A. Aragï *et al.*, *Antennas and propagation for wireless communication systems*. John Wiley & Sons, 2007.

[9] A. Goldsmith, *Wireless communications*. Cambridge university press, 2005.

[10] D. Tse and P. Viswanath, *Fundamentals of wireless communication*. Cambridge university press, 2005.

[11] L. S. Muppirisetty, T. Svensson, and H. Wymeersch, "Spatial wireless channel prediction under location uncertainty," *IEEE Transactions on Wireless Communications*, vol. 15, no. 2, pp. 1031–1044, 2016.

© 2021 IEEE. Personal use of this material is permitted. Permission from IEEE must be obtained for all other uses, in any current or future media, including reprinting/republishing this material for advertising or promotional purposes, creating new collective works, for resale or redistribution to servers or lists, or reuse of any copyrighted component of this work in other works.